Repeating 3-body collisions in a trap and the evaluation of interactions of neutral particles

C. G. Bao

Center of Theoretical Nuclear Physics, National Laboratory of Heavy Ion Collisions, Lanzhou, 73000, P.R. China
State Key Laboratory of Optoelectronic Materials and Technologies,
Sun Yat-Sen University, Guangzhou, 510275, P.R. China

A model of a device is proposed and related theoretical calculation is performed to study the weak interactions among neutral atoms and molecules. In this model 3-body collisions among the neutral particles occur repeatedly in a trap. Results of calculation demonstrate that information on interaction can be obtained by observing the time-dependent densities of the system.

I. INTRODUCTION

An important way to understand the interactions among particles is via the study of scattering. In related experiments, the initial status of a scattering state is required to be precisely controlled. This is relatively easy for charged incident particles because their initial momentum can be tuned by adjusting the electromagnetic forces imposing on them. For neutral incident particles, the initial momentum is in general difficult to control precisely. However, the recent progress in the technology of trapping neutral atoms via optical trap might open a new way for studying the scattering of neutral particles with precisely controllable initial status [1–3]. In this paper a model of a device is proposed and related theoretical calculation is performed to show how the mentioned scattering is realized. It turns out that in this device, as we shall see, the collisions among particles occur regularly and repeatedly. Thereby the effect of each individual collision can be accumulated. This would be helpful for the understanding of the very weak interactions among neutral atoms (molecules).

Traditionally, the scatterings would at most have two incident channels (say, in the experiments with head-on colliders). However, in the following device, three or more incident channels can be realized. As an example, a three-body scattering with three incident channels is chosen to be studied. This is a generalization of a previous work on a two-body scattering in a trap with two incident channels [4].

It is assumed that, in the beginning, there are three narrow optical traps located at the three vertexes of a regular triangle, and each optical trap provides a harmonic confinement. The total potential is $U_p(\mathbf{r}) = \frac{1}{2}M\omega_p^2 \sum_{j=1}^{3} |(\mathbf{r} - \mathbf{a}_j)|^2$, where $\mathbf{a}_j$ points from the origin to the $j-th$ vertexes, and M is the mass of a particle. When the center of the triangle is placed at the origin, $|\mathbf{a}_j| = a$. It is further assumed that each trap contains an atom in the ground state of a harmonic oscillator, the three atoms are identical bosons with spin zero, and ω_p is large enough so that the atoms are well localized initially. Suddenly the three narrow traps are cancelled. Instead, a broader new trap located at the

origin $U_{evol}(r) = \frac{1}{2}M\omega^2 r^2$ is created, $\omega < \omega_p$. Then, the system begins to evolve. The evolution is affected not only by $U_{evol}(r)$ but also by the atom-atom interaction $V(|\mathbf{r}_i - \mathbf{r}_j|)$. In what follows the details of the evolution is studied, three-body head-on collisions occurring repeatedly are found, and the effect of interaction is demonstrated.

II. INITIAL STATE

We shall use $\hbar\omega$ and $\sqrt{\hbar/M\omega}$ as units of energy and length. The symmetrized and normalized initial state

$$
\Psi_I = \frac{1}{\sqrt{6}}(\frac{\eta}{\pi})^{9/4}
$$
$$
\times \sum_P e^{-\frac{\eta}{2}(|\mathbf{r}_{p_1} - \mathbf{a}_1|^2 + |\mathbf{r}_{p_2} - \mathbf{a}_2|^2 + |\mathbf{r}_{p_3} - \mathbf{a}_3|^2)} \quad (1)
$$

where $\sum_P$ implies a summation over the permutations $p_1 p_2 p_3$, and $\eta = \omega_p/\omega$. Without loss of generality, $\mathbf{a}_3$ is given lying along the Z-axis, while the triangle is given lying on the X-Z plane. For convenience, three sets of Jacobi coordinates denoted by α, β, and γ, respectively, are introduced. The coordinates of the α set are defined as, $\mathbf{r} = \mathbf{r}_2 - \mathbf{r}_1$, $\mathbf{R} = \mathbf{r}_3 - (\mathbf{r}_1 + \mathbf{r}_2)/2$, and $\mathbf{R}_c = (\mathbf{r}_1 + \mathbf{r}_2 + \mathbf{r}_3)/3$. The other two sets can be obtained from the α set by cyclic permutations. In terms of the α set, we introduce the harmonic oscillator (h.o.) states $\phi_{nlm}^{(\mu)}(\mathbf{s}) \equiv f_{nl}^{(\mu)}(s)Y_{lm}(\hat{s})$ as basis functions, where $\mathbf{s} = \mathbf{r}$, $\mathbf{R}$, or $\mathbf{R}_c$. They are normalized eigenstates of the Hamiltonian $-\frac{1}{2\mu}\nabla_{\mathbf{S}}^2 + \frac{1}{2}\mu S^2$ with the eigenenergy $2n + l + 3/2$ and with the angular momentum l and its Z-component m, where $\mu = 1/2$, $2/3$, and 3 when $\mathbf{s} = \mathbf{r}$, $\mathbf{R}$, and $\mathbf{R}_c$, respectively. Then the initial state can be expanded as

$$
\Psi_I = \frac{1}{\sqrt{6}} \sum_{N_c} c_{N_c} \phi_{N_c00}^{(3)}(\mathbf{R}_c) \cdot \sum_{J,m,\Pi,q} G_{Jm\Pi q}\Phi_{Jm\Pi q}(\mathbf{r}, \mathbf{R})
$$

(2)

where the first factor is for the c.m. motion which is completely separated from the internal motion,

$$
c_{N_c} = \sqrt{4\pi}(\frac{\eta}{\pi})^{9/4} \int R_c^2 dR_c f_{N_c0}^{(3)}(R_c)e^{-\frac{3\eta}{2}R_c^2} \quad (3)
$$

The notation q denotes a set of quantum numbers n, l, N and L, and $\Pi = (-1)^{l+L}$ is the parity,

$$\Phi_{Jm\Pi q}(\mathbf{r}, \mathbf{R}) \equiv [\phi_{nl}^{(1/2)}(\mathbf{r})\phi_{NL}^{(2/3)}(\mathbf{R})_{Jm}] \qquad (4)$$

where l and L are coupled to J and m.

$$G_{Jm\Pi q} = \sum_{q'} a_{n'l'm}b_{N'L'}C_{l'm,L'0}^{Jm}(1+(-1)^{l'})$$
$$\times[\delta_{qq'} + \mathcal{A}_q^{q'J}(\beta \to \alpha) + \mathcal{A}_q^{q'J}(\gamma \to \alpha)] \quad (5)$$

where

$$a_{nlm} = \int r^2 dr \; f_{nl}^{(1/2)}(r) \; e^{-\frac{\eta}{4}r^2}$$
$$\times \int d\widehat{r} \; Y_{lm}^*(\widehat{r}) e^{\frac{\eta}{2}(\sqrt{3}\arcsin\theta_r \cos\phi_r - 3a^2/2)} \quad (6)$$

$$b_{NL} = \int R^2 dR \; f_{NL}^{(2/3)}(R) \; e^{-\frac{\eta}{3}R^2}$$
$$\times \int d\widehat{R} \; Y_{L0}^*(\widehat{R}) e^{\eta(\arccos\theta_R - 3a^2/4)} \quad (7)$$

$C_{l'm,L'0}^{Jm}$ is the Clebsch-Gordan coefficients, q' is for the set n', l', N' and L' to be summed up, θ_r and ϕ_r are the spherical polar coordinates of $\mathbf{r}$, and so on.

$$\mathcal{A}_q^{q'J}(\beta \to \alpha) \equiv \langle \; [\phi_{nl}^{(1/2)}(\mathbf{r})\phi_{NL}^{(2/3)}(\mathbf{R})]_J \; | \; [\phi_{n'l'}^{(1/2)}(\mathbf{r}^\beta)\phi_{N'L'}^{(2/3)}(\mathbf{R}^\beta)]_J \; \rangle \qquad (8)$$

is the bracket of transformation between the $\beta-$ and $\alpha-$sets (the superscript α is usually ignored), which is called the Talmi-Moshinsky (T-M) coefficients. Their analytical expression can be found in [5–7]. In general, the symmetrization would cause the appearance of all three set of coordinates. However, by using the T-M coefficients, Eq. (2) contains only the $\alpha-$set so as to facilitate greatly the calculation. Incidentally, since Ψ_I is symmetrized, l (included in q) of Eq. (2) must be even and therefore $(-1)^L = \Pi$. In principle, the right side of Eq. (2) should contain infinite terms. However, the overlap between Ψ_I and higher h.o. states are very small. Say, if, n, N, N_c are all smaller than 12 and l, L, L_c are all smaller than 23, with the parameters specified below, the overlap of the right side of Eq. (2) with itself is equal to 0.99997. This implies that higher h.o. states can be safely ignored.

III. HAMILTONIAN AND ITS EIGENSTATES

The evolution is governed by the Hamiltonian H_{evol} containing $U_{evol}(r)$ and the interaction. When the Jacobi coordinates are used it can be separated as

$$H_{evol} = H_c + H_{in} \qquad (9)$$

where $H_c = -\frac{1}{6}\nabla_{\mathbf{R}_c}^2 + \frac{3}{2}R_c^2$ describes the c.m. motion, and

$$H_{in} = -\nabla_{\mathbf{r}}^2 + \frac{1}{4}r^2 - \frac{3}{4}\nabla_{\mathbf{R}}^2 + \frac{1}{3}R^2 + \sum_{i<j}V(|\mathbf{r}_i - \mathbf{r}_j|) \quad (10)$$

describes the internal motion. Since the eigenstates of H_c are well known, if the eigenstates of H_{in} are also know, the evolution starting from any initial state can be understood. In what follows, the symmetrized eigenstates are obtained via a diagonalization of H_{in} in a limited space. In this way, only approximate solutions can be obtained. Then, we increase the dimension of the space until a better convergency is achieved.

When $\Phi_{Jm\Pi q}(\mathbf{r}, \mathbf{R})$ as defined in Eq. (4) are used as basis functions (where l is restricted to be even as mentioned), the matrix elements of H_{in} is

$$\langle \; \Phi_{J'm'\Pi'q'}(\mathbf{r}, \mathbf{R})| \; H_{in} \; | \; \Phi_{Jm\Pi q}(\mathbf{r}, \mathbf{R}) \; \rangle$$
$$= \delta_{J'J}\delta_{m'm}\delta_{\Pi'\Pi} \; [\; \delta_{q'q}(2n + 2N + l + L + 3) + \delta_{l'l}\delta_{N'N}\delta_{L'L}V_{n'nl}$$
$$+2 \sum_{q'',q'''} \delta_{l'''l''}\delta_{N'''N''}\delta_{L'''L''}\mathcal{A}_{q'''}^{q'J}(\alpha \to \beta)\mathcal{A}_{q''}^{qJ}(\alpha \to \beta) \; V_{n'''n''l''} \;] \qquad (11)$$

where q'' denotes the set $(n''l''N''L'')$, and the implication of q''' is alike,

$$V_{n'nl} = \int r^2 dr \; f_{n'l}^{(1/2)}(r) \; V(r) f_{nl}^{(1/2)}(r) \qquad (12)$$

To control the size of the space, a number N_0 is introduced and $2n + 2N + l + L \leq N_0$ is required for all the basis functions. There are two choices to obtain symmetrized eigenstates of H_{in}. In the first choice, the set $\Phi_{Jm\Pi q}(\mathbf{r}, \mathbf{R})$ is firstly symmetrized and orthonormalized before carrying on the diagonalization. However, this procedure is complicated. Therefore we make the second choice, in which the set $\Phi_{Jm\Pi q}(\mathbf{r}, \mathbf{R})$ is simply used without symmetrization but with the requirement that l must be even and all the basis functions satisfying $2n + 2N + l + L \leq N_0$ are included without missing. This requirement assures that the space is close under permutations, and no basis functions that will contribute to the symmetrized eigenstates would be missed, unless they are too high to have $2n + 2N + l + L > N_0$. However, in this choice, a number of unphysical eigenstates with confused symmetry will emerge together with those with correct symmetry. Therefore a discrimination is needed as shown below.

Let an eigenstate be denoted as $\Psi_{Jm\Pi i}$ where i is a serial number of the $Jm\Pi-$series. Expanding in terms of the basis functions,

$$\Psi_{Jm\Pi i} = \sum_q \mathcal{B}_{iq}^{Jm\Pi} \Phi_{Jm\Pi q}(\mathbf{r}, \mathbf{R}) \qquad (13)$$

where the l in q must be even, and the coefficients $\mathcal{B}_{iq}^{Jm\Pi}$ can be directly known from the diagonalization of H_{in}. If $\Psi_{Jm\Pi i}$ is correctly symmetrized, the coefficients would obey

$$\sum_q \mathcal{B}_{iq}^{Jm\Pi} \mathcal{A}_{q'}^{qJ}(\beta \rightarrow \alpha) = \mathcal{B}_{iq'}^{Jm\Pi},$$
$$\text{(for all the } q' \text{ with } l' \text{ even)} \qquad (14)$$

and

$$\sum_q \mathcal{B}_{iq}^{Jm\Pi} \mathcal{A}_{q'}^{qJ}(\beta \rightarrow \alpha) = 0, \quad \text{(for all the } q' \text{ with } l' \text{ odd)}$$
$$(15)$$

In the summations of Eqs. (14) and (15), l (in q) is restricted to be even. With the help of Eqs. (14) and (15), the states with confused symmetry can be discriminated and dropped, and all the symmetrized eigenstates under the restriction caused by N_0 can be extracted without missing. They are one-to-one identical to those obtained via the first choice if the same N_0 are used. In what follows $\Psi_{Jm\Pi i}$ denotes only the symmetrized eigenstate, and the associated energy is denoted by $E_{J\Pi i}$.

IV. EVOLUTION AND THE REPEATING 3-BODY COLLISIONS

With the eigenstates it is straight forward to obtain the time-dependent solution of H_{evol} as

$$\Psi(t) = e^{-iH_{evol} \ \tau} \Psi_I \equiv \Psi_c(\mathbf{R}_c, t) \Psi_{in}(\mathbf{r}, \mathbf{R}, t) \qquad (16)$$

$$\Psi_c(\mathbf{R}_c, t) = \frac{1}{\sqrt{6}} \sum_{N_c} c_{N_c} e^{-i\tau(2N_c + 3/2)} \ \phi_{N_c 00}^{(3)}(\mathbf{R}_c) \quad (17)$$

$$\begin{aligned}
\Psi_{in}(\mathbf{r}, \mathbf{R}, t) &= \sum_{J,m,\Pi,q} G_{Jm\Pi q} \sum_i e^{-i\tau E_{J\Pi i}} \\
&\times | \ \Psi_{Jm\Pi i} \ \rangle \langle \ \Psi_{Jm\Pi i} \ | \ \Phi_{Jm\Pi q} \rangle \\
&= \sum_{J,m,\Pi,q'} \mathcal{D}_{q'}^{Jm\Pi}(t) \ \Phi_{Jm\Pi q'}(\mathbf{r}, \mathbf{R}) \quad (18)
\end{aligned}$$

where

$$\mathcal{D}_{q'}^{Jm\Pi}(t) = \sum_{i,q} G_{Jm\Pi q} e^{-i\tau E_{J\Pi i}} \ \mathcal{B}_{iq}^{Jm\Pi} \mathcal{B}_{iq'}^{Jm\Pi} \qquad (19)$$

and $\tau = \omega t$. Obviously, Eqs. (16) to (18) give only an approximate solution because the set $\Psi_{Jm\Pi i}$ obtained via diagonalization each would deviate more or less from the corresponding exact eigenstate, and because only finite number of $\Psi_{Jm\Pi i}$ are used in the expansion. However, it is believed that, when the number of basis functions becomes larger and larger, the above $\Psi(t)$ would be closer and closer to the exact solution. The crucial point is the convergency. In this paper the interaction is assumed to be weak. It turns out that, in this case, the convergency is satisfying as shown below.

We shall demonstrate that the evolution is a repeating 3-body collisions, and the effect of interaction will be also shown. For these purposes, we extract the following quantities from $\Psi(t)$.

(i) The density $\rho_r(r,t) \equiv \int d\Omega_r \Psi^*(t)\Psi(t)$, where the integration covers all the degrees of freedom except dr. Therefore $\int dr \ \rho_r(r,t) = 1$. Obviously, $\rho_r(r,t)$ is the probability density that the inter-distance is r.

(ii) The density $\rho_R(R,t)$ fulfilling $\int dR \ \rho_R(R,t) = 1$

(iii) The density $\rho_\theta(\theta,t)$ fulfilling $\int \sin\theta \cdot d\theta \ \rho_\theta(\theta,t) = 1$, where θ is the angle between $\mathbf{r}$ and $\mathbf{R}$.

(iv) The density $\zeta(\mathbf{R},t)$ fulfilling $\int d\mathbf{R} \ \zeta(\mathbf{R},t) = 1$.

It was found that the c.m. is distributed very close to the origin, therefore $\mathbf{R}$ is approximately proportional to $\mathbf{r}_3$. Therefore, the behavior of the particle 3 can be roughly understood via $\zeta(\mathbf{R},t)$. Incidentally, the behaviors of all the particles are the same due to the symmetrization. The analytical expression of these densities are given in the appendix.

In order to have numerical results, as an example, the interaction is assumed to be a repulsive core as $V(r) = V_0$ if $r \leq 0.4$, or zero if $r > 0.4$, where V_0 is a constant to be given. The other parameters are chosen as $\eta = 1.5$, $|\mathbf{a}| = 1.5$, and $N_0 = 20$. To show the initial localization of the particles, we define the one-body density of the initial state as $\rho_1(\mathbf{r}_1) \equiv \int d\mathbf{r}_2 d\mathbf{r}_3 \Psi_I^* \Psi_I$. This density is plotted in Fig.1. Starting from Ψ_I, the details of evolution are given as follows.

$\rho_R(R,t)$, $\rho_r(r,t)$, and $\rho_\theta(\theta,t)$ against t in the earliest stage of evolution is plotted in Fig2a to 2c. Where $V_0 = 0.08$ is assumed, and ωt is from 0 to 2π (say, if $\omega = $
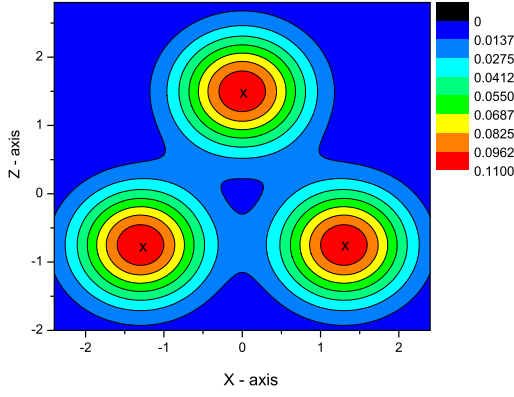
FIG. 1: Contour diagram of the one-body density $\rho_1(\mathbf{r}_1)$ of the initial state plotted in the X-Z plane. $\eta = 1.5$ and $|\mathbf{a}| = 1.5$ are adopted. Each maximum is marked with a $\times$. The three particles form a regular triangle with side-length ~ 2.6 initially. (Color online)
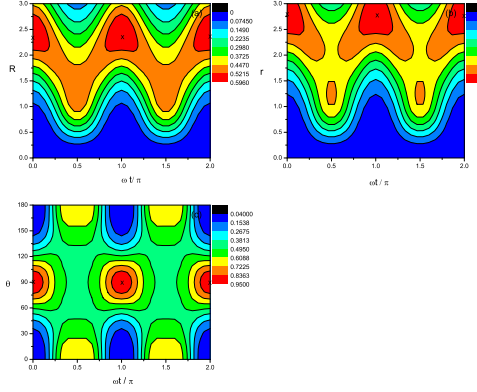

FIG. 2: Contour plots of $\rho_R(R,t)$, $\rho_r(r,t)$, and $\rho_\theta(\theta,t)$ given in (a), (b), and (c), respectively, with $\eta = 1.5$, $|\mathbf{a}| = 1.5$, $V_0 = 0.08$ and $N_0 = 20$. Each maximum is marked with a $\times$. (Color online)

$1000 \times 2\pi$, then t is from 0 to $0.001\,\text{sec}$). When $t = 0$, the inter-distances among the particles are about 2.6 as shown in Fig.1 and 2b. When the evolution begins, the peaks of ρ_r and ρ_R move inward synchronously, while ρ_θ remains to peak at $90°$. It implies a contraction of the regular triangle. Accordingly, the three particles rush towards the center leading to a 3-body head-on collision. When ωt is close to $\pi/2$, the inter-distances become much shorter, and ρ_θ becomes nearly uniform. It implies that the geometric character (i.e., the regular triangle) will be spoiled when the particles are close to each other.

After the first collision, the particles move outward. When $\omega t = \pi$, each particle will be close to the opposite end of its initial position as shown by the solid curve of Fig.3a. Where $\zeta(\mathbf{R},t)$ is given at the point $\mathbf{R} \equiv (R, \theta_R, \phi_R) = (2.25, \pi, 0)$ and ωt is given in the interval $[0, 2\pi]$. The sharp peak of the solid curve demonstrates clearly that a particle arrives at the opposite end when $\omega t \sim \pi$. Due to the symmetrization of the wave
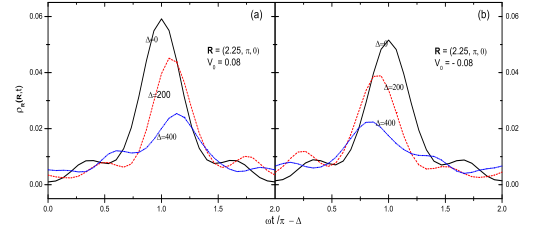

FIG. 3: $\zeta(\mathbf{R},t)$ against t given in three selected intervals of t. $\mathbf{R}$ is fixed at $(2.25, \pi, 0)$ (i.e., $\mathbf{R}$ is lying along the negative Z-axis with $R = 2.25$. Meanwhile particle 3 is close to the opposite end of the up-vertex of the initial triangle). The three curves are associated with the three choices of Δ, namely, 0, 200, and 400. When $\Delta = 0$, the interval of ωt is $[0, 2\pi]$ (solid curve). When $\Delta = 200$, it is $[200\pi, 202\pi]$ (dash curve). When $\Delta = 400$, it is $[400\pi, 402\pi]$ (dash-dot-dot curve). $V_0 = 0.08$ (a) and -0.08 (b). The other parameters are the same as in Fig.2. (Color online)

function, this is also true for other two particles. Then, the above process begins to reverse. When $\omega t = 2\pi$, the system recovers its initial status nearly. If the interaction is removed, the recovery is complete and the system will undergo an exact periodic motion with the period $2\pi/\omega$. The motion is characterized by the repeating head-on 3-body collisions. each occurs once within the interval π/ω.

However, due to the interaction, the recovery is not exact. When the time goes on the effect of the weak interaction will accumulate and gradually emerge. This is shown by the dash-curve of Fig.3a which describes the behavior of $\zeta(\mathbf{R},t)$ after 200 rounds of head-on collisions. Where the peak is lower than that of the solid curve. It implies that the density is diffusing. Furthermore, the peak of the dash-curve has shifted a little right implying that the arrival is a little delayed. The diffusion and the delay will become more explicit when t is larger as shown by the dash-dot-dot curve. When the interaction is attractive, the above repeating 3-body collisions remain, and the densities remain to be diffusing. However, instead of a delay, the peak will arrive at the end earlier as shown in Fig.3b, where $V_0 = -0.08$. Due to the diffusion of the density as shown in Fig.3, the phenomenon of repeating 3-body collisions will become ambiguous when t is sufficiently large.

When V_0 is given at a number of values and $\mathbf{R}$ is fixed at $(2.25, \pi, 0)$, $\zeta(\mathbf{R},t)$ against ωt is plotted in Fig.4, in which ωt varies in an interval close to 201π. In this figure both the locations and the heights of the peaks depend on the strength V_0. In general, a larger $|V_0|$ will cause a stronger diffusion and therefore a shorter life of the phenomenon of clear repeating 3-body collisions, and a more positive (negative) V_0 will cause a larger shift of the peak to the right (left). In addition to V_0, the evolution depends also on the range of interaction. Therefore, by observing the time-dependent densities, information on the interaction can be obtained.
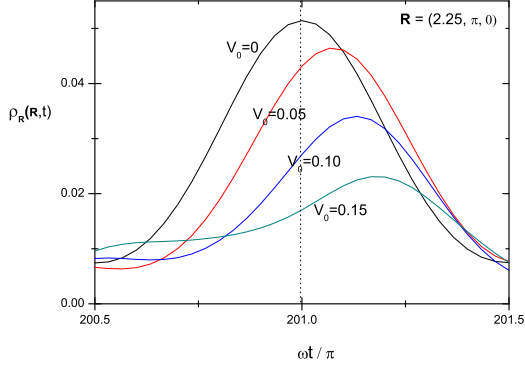
FIG. 4: $\zeta(\mathbf{R}, t)$ against t in an interval close to $201\pi/\omega$. $\mathbf{R}$ is fixed at $(2.25, \pi, 0)$. V_0 is given at four values marked by the curves. The other parameters are the same as in Fig.2. (Color online)

The accuracy of the above numerical results depends on N_0, the number controlling the total number of basis functions. As an example the values of $\zeta(\mathbf{R}, t)$ are listed in Table 1 to show the dependence.

TABLE I: The values of $\zeta(\mathbf{R}, t)$ with $\mathbf{R} = (2.25, \pi, 0)$ and with three choices of N_0. The other parameters are the same as those for Fig.2

N_0	16	20	24
$\zeta(\mathbf{R}, 31\pi/\omega)$	0.0590	0.0586	0.0586
$\zeta(\mathbf{R}, 91\pi/\omega)$	0.0547	0.0542	0.0543
$\zeta(\mathbf{R}, 151\pi/\omega)$	0.0472	0.0468	0.0469

The convergency shown in this table is satisfying. Thus we conclude that the numerical results obtained by using $N_0 = 20$ are accurate enough in qualitative sense.

V. SUMMARY

A model of a device containing repeating 3-body collisions is proposed to study the weak interactions among neutral atoms and molecules. The advantage is twofold. (i) The initial status can be precisely controlled. (ii) The weak effect of the interaction can be accumulated and therefore easier to be detected. Numerical results support that information on interaction can be thereby extracted.

A crucial point in the device is the initial localization of the particles. If they are better localized (by increasing ω_p) and/or they are more separated from each other initially (by increasing $|\mathbf{a}_j|$), the repeating 3-body collisions would become more explicit and be maintained longer. Furthermore, if H_{evol} has a larger ω, the interval between two successive collisions ($\sim \pi/\omega$) becomes shorter, therefore the evolution would proceed swifter.

Although the three particles are assumed to be identical bosons, a generalization to fermions and/or distinguishable particles is straight forward. In principle, the above device could also be used to study the three-body forces if they exist.

Appendix A: Analytical expressions of the time-dependent densities

The analytical expressions of the time-dependent densities are as follows.

(i)
$$\rho_R(R, t) = \frac{1}{6} \sum_{N_c} (c_{N_c})^2 \sum_{J, m, \Pi, q', q} \delta_{n'n} \delta_{l'l} \delta_{L'L}$$
$$\times [\mathcal{D}_{q'}^{Jm\Pi}(t)]^* \ \mathcal{D}_q^{Jm\Pi}(t)$$
$$\times R^2 f_{N'L}^{(2/3)}(R) f_{NL}^{(2/3)}(R) \tag{A1}$$

(ii)
$$\rho_r(r, t) = \frac{1}{6} \sum_{N_c} (c_{N_c})^2 \sum_{J, m, \Pi, q', q} \delta_{N'N} \delta_{l'l} \delta_{L'L}$$
$$\times [\mathcal{D}_{q'}^{Jm\Pi}(t)]^* \ \mathcal{D}_q^{Jm\Pi}(t)$$
$$\times r^2 f_{n'l}^{(1/2)}(r) f_{nl}^{(1/2)}(r) \tag{A2}$$

(iii) For the derivation of $\rho_\theta(\theta, t)$, a transformation is made so that $\mathbf{r}$ and $\mathbf{R}$ are transformed to r, R, θ, and the three Euler angles specifying the orientation of the triangle formed by the three particles. Then, integrating all the degrees of freedom except θ, we have

$$\rho_\theta(\theta,t) = \frac{1}{6}\sum_{N_c}(c_{N_c})^2 \sum_{J,m,\Pi',\Pi,q',q}[\mathcal{D}_{q'}^{Jm\Pi'}(t)]^* \, \mathcal{D}_q^{Jm\Pi}(t)\,(-1)^{l+l'-J}$$

$$\times[(2L'+1)(2L+1)(2l'+1)(2l+1)]^{1/2}\,[\int r^2 dr\, f_{n'l'}^{(1/2)}(r)\,f_{nl}^{(1/2)}(r)]$$

$$\times[\int R^2 dR\, f_{N'L'}^{(2/3)}(R)\,f_{NL}^{(2/3)}(R)]$$

$$\times\sum_\lambda W(ll'LL';\lambda J)\sqrt{\frac{\pi}{2\lambda+1}}C_{L0,L'0}^{\lambda 0}C_{l0,l'0}^{\lambda 0}Y_{\lambda 0}(\theta,0) \tag{A3}$$

where the Wigner and Clebsch-Gordan coefficients are introduced.

$$\text{(iv)}\ \zeta(\mathbf{R},t) = \frac{1}{6}\sum_{N_c}(c_{N_c})^2 \sum_{J',J,m',m,\Pi',\Pi,q',q}\delta_{n'n}\delta_{l'l}[\mathcal{D}_{q'}^{J'm'\Pi'}(t)]^* \, \mathcal{D}_q^{Jm\Pi}(t)$$

$$\times\sum_k[C_{l'k,L'm'-k}^{J'm'}C_{lk,Lm-k}^{Jm}Y_{L',m'-k}^*(\widehat{R})Y_{L,m-k}(\widehat{R})]$$

$$\times f_{N'L'}^{(2/3)}(R)\,f_{NL}^{(2/3)}(R) \tag{A4}$$

[1] Stenger, J., Inouye, S., Stamper-Kurn, D. M., Miesner, H.-J., Chikkatur, A. P., Ketterle, W.: Spin domains in ground-state Bose-Einstein condensates. Nature (London) **396**, 345 (1998).
[2] Barrett, M. D., Sauer, J. A., Chapman, M. S.: All-Optical Formation of an Atomic Bose-Einstein Condensate. Phys. Rev. Lett. **87**, 010404 (2001).
[3] Würtz, P., Langen, T., Gericke, T., Koglbauer, A., Ott, H.: Experimental Demonstration of Single-Site Addressability in a Two-Dimensional Optical Lattice. Phys. Rev. Lett. **103**, 080404 (2009).
[4] Li, Z. B., Chen, Z. F., He, Y. Z., Bao, C. G.: Evaluation of the $^{52}Cr-^{52}Cr$ interaction via repeating collisions of a pair of atoms in a trap. preprint, arXiv:0908.2929v1.
[5] Tobocman, W.: A generalized Talmi-Moshinsky transformation for few-body and direct interaction matrix elements. Nucl. Phys. A. **357**, 293 (1981).
[6] M. Baranger, M., Davies, K. T. R.: Oscillator brackets for Hartree-Fock calculations. Nucl. Phys. **79**, 403 (1966).
[7] Brody, T. A., Moshinski, M.: Table of Transformation Brackets. Monografias del Instituto de Fisica, Universidad Nacional Autonoma de Mexico (1960).